ACS NANO

www.acsnano.org

ARTICLE

Resolving the Structure of a Well-Ordered Hydroxyl Overlayer on $In_2O_3(111)$: Nanomanipulation and Theory

Margareta Wagner,*[,†] Peter Lackner,[†] Steffen Seiler,[‡] Achim Brunsch,[‡] Roland Bliem,[†] Stefan Gerhold,[†] Zhiming Wang,[†] Jacek Osiecki,[§] Karina Schulte,[§] Lynn A. Boatner,[∥] Michael Schmid,[†] Bernd Meyer,[‡] and Ulrike Diebold[†]

[†]Institute of Applied Physics, TU Wien, Wiedner Hauptstraße 8-10/134, 1040 Vienna, Austria

[‡]Interdisciplinary Center for Molecular Materials and Computer-Chemistry-Center, Friedrich-Alexander-Universität Erlangen-Nürnberg, Nägelsbachstraße 25, 91052 Erlangen, Germany

[§]MAX IV Laboratory, Lund University, Ole Römers väg 1, 223 63 Lund, Sweden

[∥]Materials Science and Technology Division, Oak Ridge National Laboratory, Oak Ridge, Tennessee 37831, United States

S *Supporting Information*

ABSTRACT: **Changes in chemical and physical properties resulting from water adsorption play an important role in the characterization and performance of device-relevant materials. Studies of model oxides with well-characterized surfaces can provide detailed information that is vital for a general understanding of water−oxide interactions. In this work, we study single crystals of indium oxide, the prototypical transparent contact material that is heavily used in a wide range of applications and most prominently in optoelectronic technologies. Water adsorbs dissociatively already at temperatures as low as 100 K, as confirmed by scanning tunneling microscopy (STM), photoelectron spectroscopy, and density functional theory. This dissociation takes place on lattice sites of the defect-free surface. While the $In_2O_3(111)$-(1 × 1) surface offers four types of surface oxygen atoms (12 atoms per unit cell in total), water dissociation happens exclusively at one of them together with a neighboring pair of 5-fold coordinated In atoms. These O−In groups are symmetrically arranged around the 6-fold coordinated In atoms at the surface. At room temperature, the $In_2O_3(111)$ surface thus saturates at three dissociated water molecules per unit cell, leading to a well-ordered hydroxylated surface with (1 × 1) symmetry, where the three water O_WH groups plus the surface O_SH groups are imaged together as one bright triangle in STM. Manipulations with the STM tip by means of voltage pulses preferentially remove the H atom of one surface O_SH group per triangle. The change in contrast due to strong local band bending provides insights into the internal structure of these bright triangles. The experimental results are further confirmed by quantitative simulations of the STM image corrugation.**

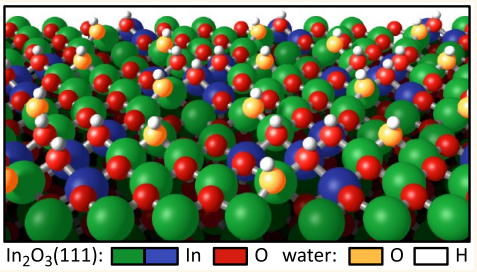

KEYWORDS: *indium oxide, water dissociation, hydroxylation, scanning tunneling microscopy, density functional theory*

The interaction of oxide surfaces with water vapor under ambient conditions plays an important role in thin-film device technology, as water adsorption or hydroxylation of the surface influence, for example, the catalytic reactivity and electronic properties. Thus, it is of paramount importance to study the interaction of water with oxide surfaces. In the past decades, the adsorption and dissociation of water at various temperatures has been intensely studied on metal-oxide surfaces, including rutile $TiO_2(110)$,[1,2] anatase $TiO_2(101)$,[3,4] $CeO_2(111)$,[5] CoO(111),[6] MgO,[7] ZnO,[8,9] and Sr_2RuO_4;[10] a recent overview of water structures on oxides is given in ref 11.

In this work, we focus on indium oxide, In_2O_3. This prototypical transparent conductive oxide (TCO) combines optical transparency in the visible range of light with electrical conductivity, although it has a fundamental band gap of 2.93 eV.[12,13] The intrinsic conductivity of this material can be enhanced by n-type doping with Sn; the doped material is commonly referred to as indium tin oxide (ITO). Reports regarding replacing ITO because of limited In sources have been recently refuted (In is a byproduct of Zn refinement with an abundance comparable to Ag), and the long-term supply appears to be secure.[14] In addition, the properties of ITO are not met by any other prospective material candidate: ITO is

Received: September 7, 2017
Accepted: November 1, 2017
Published: November 1, 2017

DOI: 10.1021/acsnano.7b06387
ACS Nano 2017, 11, 11531−11541

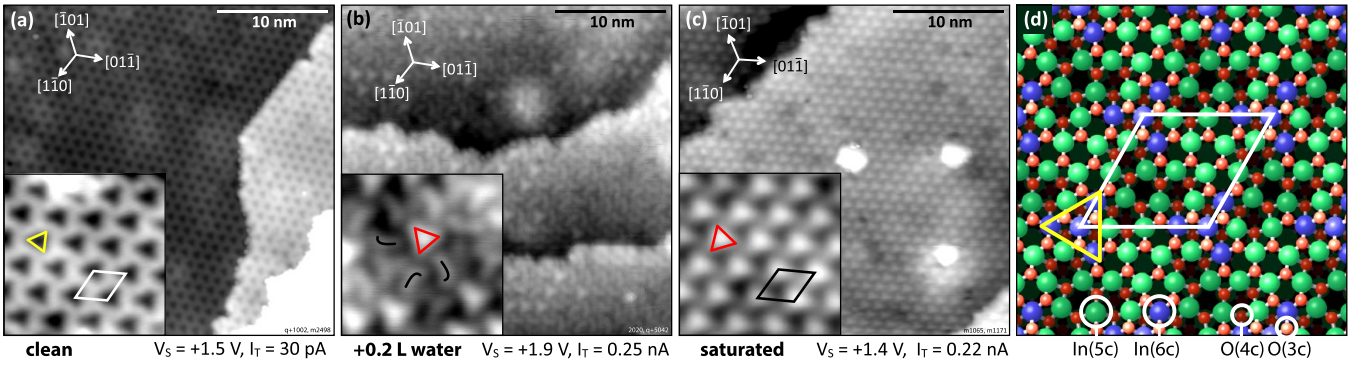

Figure 1. STM on $In_2O_3(111)$. (a) Clean surface, (b) after exposure to 0.2 L, and (c) saturated with water at room temperature. The position in the unit cell and the orientation of the dark triangular features characteristic of the clean surface are marked in the inset of (a) with a yellow triangle. The orientation of the bright water-related feature is highlighted with red triangles in the insets of (b,c). (d) Atomic structure of the stoichiometric $In_2O_3(111)$ surface (confirmed by DFT[29]). T_{STM} = (a) 5 K, (b) RT, and (c) 79 K.

suitable for thin film growth, and it excels over other TCOs such as doped SnO_2 or ZnO.[15] As such, ITO is currently widely used as a contact electrode in liquid crystal displays and solar cells,[16] and recently, it is also of increasing interest as a sensor and catalytic material.[17,18] Thus, it seems that indium oxide will remain the TCO material of choice for the foreseeable future.

Previous studies of water adsorption on In_2O_3 were mainly conducted using photoelectron spectroscopy. On the clean surface, side peaks and shoulders on the high binding energy side of the O1s core level signal were assigned to oxygen in the vicinity of bulk oxygen vacancies and hydroxyl groups on the surface. After water/air exposure, the new peak at 532−532.5 eV was variably assigned to hydroxyl groups at the surface, "water-related species", and physisorbed oxygen. The different interpretations might be due to the variety of samples used, including single crystals and (un)doped thin films as well as nanoparticles and powders.[19−27]

The present investigation has been conducted on In_2O_3 single crystals exposing the (111) surface. This nonpolar thermodynamically most stable facet[28] is principally present in nanoparticles and powders. The surface was thoroughly characterized previously.[29] In the stoichiometric form that is achieved under oxidizing preparation conditions, the material exhibits a simple (1 × 1) surface structure, with some pronounced relaxations from the truncated bulk. Reducing the surface results in single In adatoms; the reduction can either be achieved thermally, by heating in ultrahigh vacuum (UHV),[29] or chemically, by doping with an impurity atom.[30] These adatoms adsorb preferentially at one specific site of the unit cell, forming an ordered array.

This paper reports on the interaction of the stoichiometric $In_2O_3(111)$ surface with small amounts of water under UHV conditions. The present investigations were carried out using scanning tunneling microscopy (STM) and X-ray photoelectron spectroscopy (XPS), as well as density functional theory (DFT) calculations. The experiments show that the $In_2O_3(111)$ surface, despite not exhibiting reactive defects such as intrinsic surface oxygen vacancies,[29] is very reactive toward water in UHV conditions, resulting in water dissociation at lattice sites already at 100 K. At room temperature (RT), the formation of a well-ordered saturation layer with a (1 × 1) structure is observed, which contains three dissociated water molecules per unit cell (*i.e.*, three terminal O_WH groups and three surface O_SH groups formed by the split-off protons). At 100 K, the dissociation of water at the interface is followed by the adsorption of molecular water.

In_2O_3 is a complex oxide with a large bulk unit cell. The hexagonal unit cell of the $In_2O_3(111)$ surface with a lattice constant of 1.431 nm contains four inequivalent types of surface oxygen atoms and 16 In atoms in two different coordinations. The four 6-fold coordinated In atoms, In(6c), of the unit cell are not evenly distributed but arranged in a close-packed triangle, bridged by three symmetry-equivalent 3-fold coordinated O atoms, O(3c), at the surface. These O atoms together with two neighboring 5-fold coordinated In atoms are involved in the water splitting and the proton and hydroxyl adsorption, thus making the unit cell inhomogeneous in terms of reactivity. Overall, the water dissociation and formation of the OH groups can be understood from the atomic arrangement of the low-coordinated O and In atoms surrounding the high-coordinated In atoms at the surface.

RESULTS

Overview: Water Adsorption at Room Temperature. Exposing the $In_2O_3(111)$ surface to water at RT quickly leads to saturation, with several different features observed in STM along the way. Figure 1 provides an overview of the clean $In_2O_3(111)$ surface, an intermediate water coverage, and the saturated surface. The clean $In_2O_3(111)$ surface is shown in Figure 1a. Characteristic dark triangles form the (1 × 1) structure. The inset in Figure 1a shows a high-resolution image. The position of these triangles relative to the surface lattice was identified previously[29] (rectifying an earlier, wrong assignment[31]). The atomic model displayed in panel (d) was confirmed by DFT calculations.[29] The In(6c) (blue) and their O(3c) neighbors (light red) of the (1 × 1) surface form the dark triangle in the STM images, which is an entirely electronic feature due to a low contribution of the In(6c) atoms to the density of states in the lower-energy range of the conduction band.[29]

When the surface is exposed to 1 Langmuir (L, where 1 L = 1.33×10^{-6} mbar s) of water at room temperature, the STM contrast changes to bright triangles; see Figure 1c. Note, however, that these bright triangles are rotated by 60° compared to the dark triangular features of the clean surface, as emphasized by the yellow and red markers in the insets in Figure 1a,c, respectively. As is shown in the following sections, each bright triangle contains three dissociated water molecules.

DOI: 10.1021/acsnano.7b06387
ACS Nano 2017, 11, 11531−11541

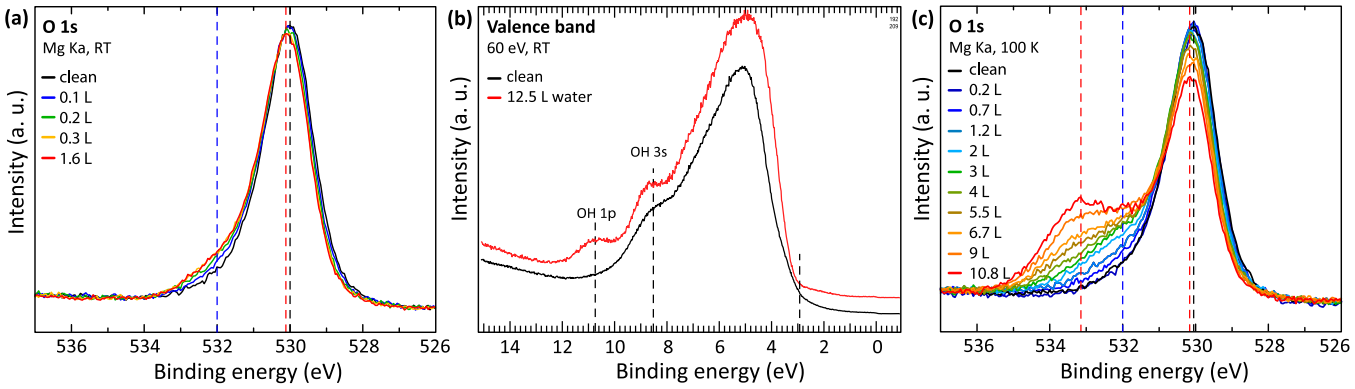

Figure 2. Grazing-emission XPS spectra of the O1s core level and the valence band during water adsorption at different substrate temperatures. (a) RT: The shoulder at high binding energies is due to hydroxylation; saturation is reached at ~0.3 L. (b) RT: Valence band spectra of the clean $In_2O_3(111)$ surface and after exposure to 12.5 L H_2O. (c) 100 K: The feature at 533.2 eV is due to molecular water. In both sets of core level spectra, a small downward band bending by ~0.12 eV is apparent upon hydroxylation of the surface.

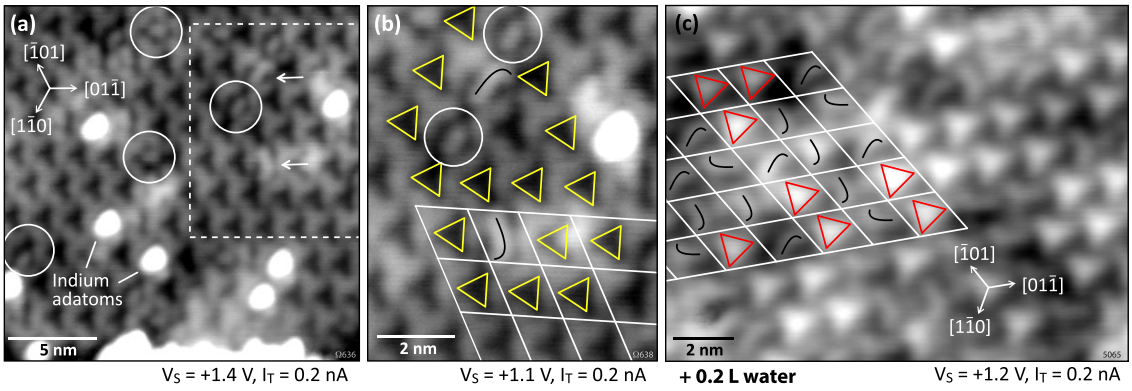

Figure 3. Very low coverages of water on $In_2O_3(111)$. (a) Partially reduced surface with few In adatoms[29] and single water-related features that appear as curves (arrows, two dissociated water molecules) and small ovals (white circles, one dissociated water molecule). (b) Zoomed image of the framed region of (a). The orientation of the curved features is indicated, as well as the dark triangles next to them. (c) After exposure to ~0.2 L at RT water, the surface is fully covered with the curved features and bright triangles (red triangles, three dissociated water molecules). The grid centering the dark triangles (as indicated in (b)) shows that both species occupy the same region within the unit cell. T_{STM} = (a,b) RT and (c) 5 K.

That the bright, rotated triangles are related to water exposure is already clear by considering an STM image taken after a somewhat smaller water dosage (Figure 1b). After dosing 0.2 L (5×10^{-9} mbar for 40 s) at room temperature, a few bright triangles are present. The surface is covered by less bright features with a curved shape, present in three orientations (marked in the inset). Below, these curved features are assigned to two dissociated water molecules; addition of a third molecule completes the structure and results in the bright triangle.

Note that the surface does not show mirror symmetry along any direction (the surface unit cell can be assigned to plane group p3). The resulting chirality of the surface is reflected in the three different, 120° rotated orientations of the curved features mentioned earlier.

XPS: Determination of Molecular *versus* Dissociated Water. To determine whether water is adsorbed molecularly or dissociatively, the STM measurements were complemented by photoelectron spectroscopy. The evolution of the O1s core level was monitored in XPS measurements following water dosages in steps of ~0.1 to 1.6 L in total (the values include codosing from the residual gas; not all of the spectra are shown here). Figure 2a displays the core level spectra of the clean surface (black) and after water exposure at room temperature. For the clean surface, the main O1s peak is located at ~530.0 eV; when water adsorbs, a small shift to higher binding energies is observed and a weak shoulder rises at ~532 eV (it should be noted that due to the high reactivity of the surface a nominally clean sample already shows the presence of water in the O1s spectrum). Saturation is reached after a dose of ~0.3 L (orange curve), spectra obtained at higher coverage [*e.g.*, 1.6 L of water (red curve)] are identical. Difference spectra are provided in the Supporting Information. The O1s shoulder is indicative of surface hydroxyls, that is, dissociated water. This assignment is supported by UPS measurements of the valence band region (Figure 2b), where the peaks corresponding to the 3σ and 1π orbitals typical of hydroxyls[32] are clearly apparent after saturating the surface with water at RT.

The XPS measurements were repeated with the sample kept at 100 K during both dosing and measurements (see Figure 2c). The total dose amounted to 10.8 L (again, including codosing from the residual gas). The main peak shifts by ~0.1 eV to higher binding energies. A shoulder at the higher binding energy side increases with exposure of water, resulting in peaks at ~532 and ~533 eV. Difference spectra are provided in the Supporting Information. By comparing the peak evolution and positions at RT and 100 K, it is evident that water dissociates at RT, resulting in a hydroxylated surface where additional water

DOI: 10.1021/acsnano.7b06387
ACS Nano 2017, 11, 11531−11541

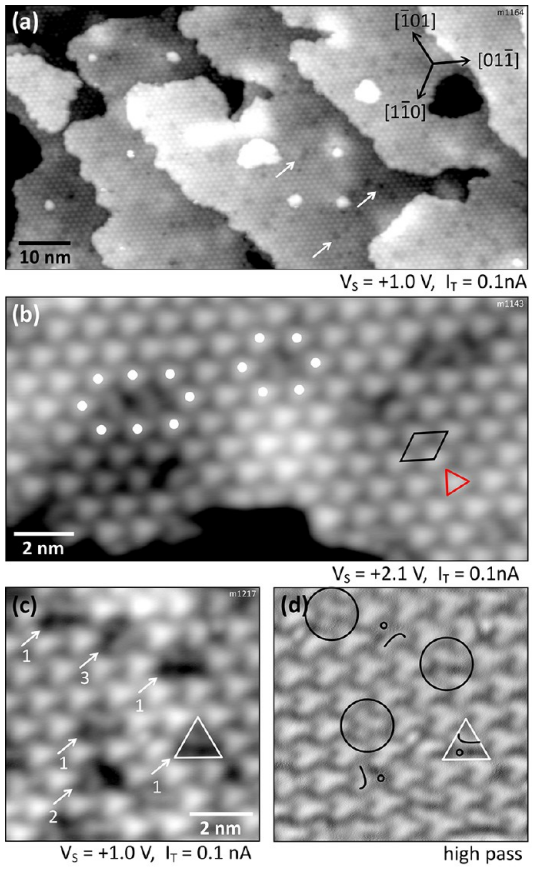

Figure 4. Fully hydroxylated In_2O_3(111) surface after dosing 1 L of water at RT. (a) Overview image with dark dots/vacancies on the terraces indicated by arrows. (b) Terrace with OH vacancies in the hydroxyl overlayer. (c) Close-up on these vacancies; some elongated species are visible inside. (d) Same image as in (c) but high-pass filtered. Symbols are explained in the main text. T_{STM} = 79 K.

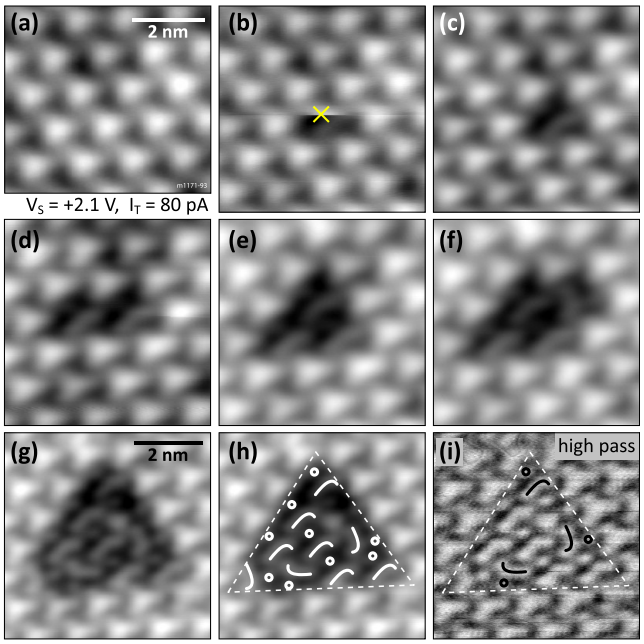

Figure 5. Manipulation of single OH groups at T = 79 K: (a–g) Applying single voltage pulses with the STM tip while scanning (the slow scanning direction is downward). The tip is placed on top of the center of the bright triangle when the pulse (+2.8 V) is triggered. The "×" in (b) marks the position where the first pulse was applied while acquiring this image. (h) Same image as in (g), indicating the species remaining on the surface. (i) High-pass filtered version of the image before for better visibility of the surface area after removing 10 hydroxyl groups. The curved features and dots are indicated.

can neither adsorb nor dissociate. At 100 K, water in direct contact with the In_2O_3(111) surface dissociates, while at higher doses, molecular water also adsorbs, possibly as multilayers. STM images of dissociated water are similar at both temperatures; molecular water could not be imaged properly due to strong interactions with the STM tip (see the Supporting Information).

Submonolayer Coverages of Water. On nominally clean In_2O_3(111) surfaces, two different features are already found in the STM images, which can be attributed to water adsorption from the residual gas in the UHV chamber. An example is given in Figure 3a on a partly reduced surface, that is, a clean surface with a few dispersed In adatoms (here, the sample was prepared by annealing the clean surface at 300 °C in UHV for 20 min, which causes a low adatom coverage[29]). Two curved features are marked with arrows in Figure 3a; note that their shape is asymmetric; the same features are present after purposely exposing the In_2O_3(111) surface to 0.2 L H_2O (see Figure 1b). In addition, several smaller, oval features (white circles) are observed in Figure 3a. The region with the curved features is enlarged in panel (b), where the dark, triangularly shaped features of the clean In_2O_3(111) surface are highlighted by yellow triangles. The curved feature can occur in three different orientations (inset Figure 1b), with their asymmetric shape resembling the letter "J" (on all terraces for a given crystal) due to the chirality of the In_2O_3(111) surface. Thus, the handedness of the surface and therefore the proper orientation of the atomic model can be easily detected by the "J" or "L" (which would reflect the other handedness) shape of these features. The small ovals (marked by white circles) are also present in three equivalent orientations (not shown here).

Knowing the position of the curved features within the unit cell makes it possible to determine the position of the bright triangles, which locally form the saturated structure. This is illustrated in Figure 3c for a surface exposed to ~0.2 L of water. The curved features cover the entire surface, together with bright triangles. Applying the same grid that centered the dark triangles in panel (b) shows that both the curved features and the bright triangles occupy the same spot in the unit cell as the dark triangles of the clean In_2O_3(111) surface. This is an indication that the curved features convert into the bright triangles upon further water dosing, and the bright triangles are above the In(6c) triangles of the substrate (but rotated differently).

STM-Tip-Induced Manipulation of the Water Layer. The curved and oval features are both immobile at 79 K and are stable when scanned with the STM up to (sample) bias voltages of +3.0 V. At higher voltages, the tip starts to interact with these features (see the Supporting Information).

Exposing the In_2O_3(111) surface at RT to >0.3 L of water leads to a saturated surface. The large-area STM image of Figure 4a was obtained after exposing the surface to 1 L of water, which is well beyond the dose required to reach saturation. However, the surface does not look uniform due to dark features that are randomly distributed across the surface.

DOI: 10.1021/acsnano.7b06387
ACS Nano 2017, 11, 11531–11541

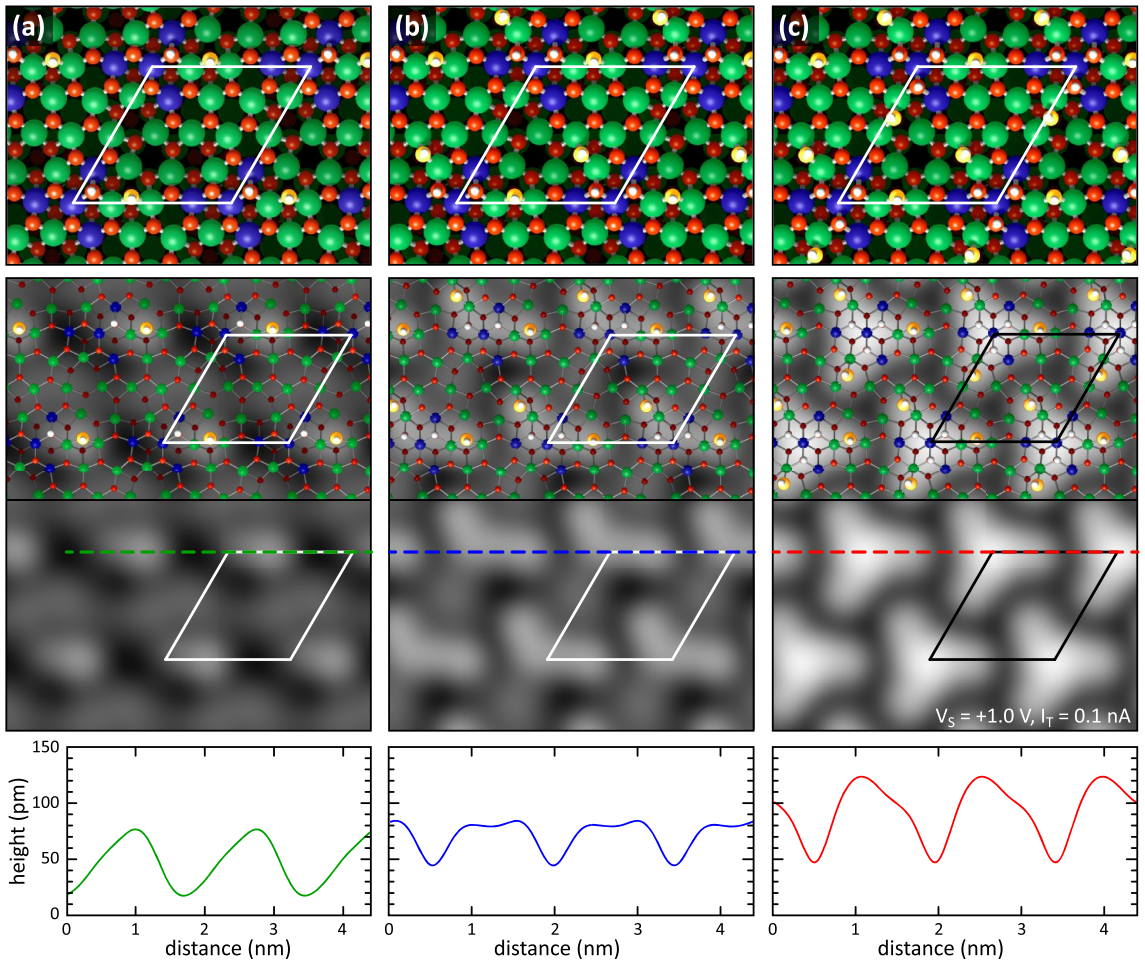

Figure 6. DFT calculations of water on In_2O_3(111). (a) One, (b) two, and (c) three dissociated water molecules per surface unit cell. The atoms of the surface are color-coded as in Figure 1. The O atom originating from the water molecule (yellow) and the hydrogen (white) are enlarged in the superimposed images for better visibility. The middle and bottom panel show the STM contrast and the apparent height in line profiles, respectively, calculated using the Bardeen approach.

The density of these dark features varies for each surface preparation, but a few were always present, especially when the sample temperature was slightly elevated (*e.g.*, after annealing during sample preparation) during the water exposure. Figure 4b presents a closer look at these dark features; they occupy the space otherwise taken by the bright triangles. To guide the eye, the nearest neighboring (n.n.) bright triangles are highlighted with white dots around a single (6 n.n.) and two adjoining (8 n.n.) dark features. The internal structure of these dark features is investigated in panel (c), where six of them are marked by arrows. The overall shape of this feature resembles a triangle (indicated in white), pointing up in the figure. Moreover, one can identify three orientations of this feature, where the somewhat brighter region is either in the top (labeled "1"), left ("2"), or right ("3") corner of the white triangle. For better visibility, a high-pass filtered version of this image is shown in Figure 4d. The white marker triangle is placed at the same position as in (c), and superimposed curved lines indicate the three orientations of the internal structure. Located at the convex side of the curve, an additional dot is always present [hardly visible in the unprocessed STM image here due to its small apparent height of ∼17 pm, marked by a small black ring (compare also Figure 5c−i)]. For a better view and comparison, these symbols are placed only on one feature of orientation "1", and the three remaining features are encircled in black in Figure 4d.

The same curved features in three orientations (without the dot) were described earlier for the surface after water exposure below the saturation dosage. Hence, it is likely that the dark features represent a partial vacancy in the saturated structure; most likely one OH group is missing.

In order to test whether these dark features are indeed partial vacancies in the saturated structure, bias pulses (+2.8 V sample bias, *i.e.*, the tip is negative) were applied to a defect-free region of the surface of Figure 4. The first three panels of Figure 5 show (a) the intact surface, (b) the image where a pulse is applied while scanning at the position marked by an ×, and the same region in a subsequent scan (c). During this sequence, one bright triangle was transformed into a dark feature/vacancy (curved feature plus dot feature). The pulses were repeated on the surrounding bright triangles until 10 of them (arranged in a large triangle) were transformed. Figure 5g−i shows in more detail the area where 10 bright triangles were transformed. (Note that there is a defect in the upper part of the transformed region, which happened after a manipulation.) In panel (h), symbols that indicate the orientations of the remaining curved species are superimposed on the STM image from panel (g). The same image is displayed in panel (i), where the contrast is enhanced by applying a high-pass filter. The curved features

DOI: 10.1021/acsnano.7b06387
ACS Nano 2017, 11, 11531−11541

have an apparent height of ~65 pm, and the dots measure ~17 pm in height and the bright triangles ~150 pm with respect to the manipulated area. The corrugation of the undisturbed hydroxylated surface is ~60 pm.

Moreover, the transformation does not only work with single voltage pulses, but it is also induced by scanning a larger area at high bias voltage, although a higher value of +3.6 V is necessary to transform the entire scanned area at once (see the Supporting Information).

DFT: Configurations of Adsorbed Water Molecules. To solve the atomic structures of the adsorbed water molecules on the $In_2O_3(111)$ surface, a series of DFT calculations was performed. First, we determined the preferred adsorption geometry of a single water molecule in the primitive (1 × 1) surface unit cell. Both molecular and dissociative configurations were considered. The calculations show that intact water molecules preferentially coordinate *via* their oxygen atom, O_W, to the unsaturated In(5c) sites, whereas upon dissociative adsorption, the proton converts an O(3c) surface oxygen, O_S, to a hydroxyl (O_SH), and the remaining O_WH group from the water molecule takes either an on-top or a bridging position at the In(5c) sites. The $In_2O_3(111)$ surface contains four nonequivalent 5-fold coordinated In(5c) and four nonequivalent 3-fold coordinated O(3c) sites per (1 × 1) surface unit cell. DFT calculations were performed for all nonequivalent sites probing both molecular and dissociative adsorption (see the Supporting Information). We find that dissociative adsorption is clearly preferred (binding energy 1.28 *versus* 0.73 eV). In the most favorable configuration (see Figure 6a), the proton adsorbs on one of the three O(3c) binding to two In(6c) and one In(5c) (*i.e.*, within the area that is imaged as a dark triangle in STM). The preference of this O(3c) site for the proton is an electronic effect, as shown by a detailed analysis in the Supporting Information. The remaining O_WH group adsorbs in a bridging position between the two In(5c) that are closest to the O_SH group. In the calculated STM image (see Figure 6a), the two O_SH and O_WH hydroxyl groups appear as a single oval-shaped protrusion.

Subsequently, a second and a third water molecule were added to the (1 × 1) surface unit cell, again probing molecular and dissociative adsorption at all nonequivalent surface sites (see the Supporting Information). In the most favorable configurations, these additional water molecules are also dissociated. They occupy the two sites that are symmetry-equivalent to the adsorption site of the first water molecule (see Figures 6b,c). In the calculated STM images, two dissociated water molecules appear as a single curved feature, and three dissociated water molecules are visible as a single bright triangle. The binding energy per molecule decreases slightly from 1.28 to 1.23 and 1.18 eV when going from one to two and three water molecules, respectively. The reason for this decrease is a small, substrate-mediated effective repulsion between the molecules due to surface re-relaxations.[33] The adsorption of water molecules leads to a partial lifting of the relaxations of the surface atoms that occurred upon cleavage of the crystal. This re-relaxation contributes to the water binding energy. However, this energy gain is available to its full extent only for the first adsorbate, and it is reduced for the second and third molecule[33] (see the Supporting Information).

Finally, when going to higher surface coverages beyond three (dissociated) molecules per unit cell, we find that for these additional molecules molecular adsorption becomes more favorable than dissociation (see the Supporting Information). The binding energy of these water molecules is more than 0.3 eV lower compared to the energy of the dissociated molecules in the saturated structure. Converting the binding energies per molecule into energy gains per area upon water adsorption and representing the results in form of a surface phase diagram[34] (see Figure 7) shows that the structure with three dissociated water molecules is the thermodynamically most stable one for a wide window in the chemical potential of water (corresponding to partial pressure conditions around UHV at RT). The higher water coverages, which include molecular water, appear as thermodynamically most stable structures only at higher chemical potentials. In UHV, they exist only well below room temperature.

Based on these DFT results, all of the features observed in the STM measurements are clearly identified. We assign (i) the bright triangles to three water molecules adsorbed dissociatively at the three symmetry-equivalent sites formed by the O(3c) and In(5c) bridges closest to the corner of the unit cell; (ii) the curved feature appearing at lower water dose to two water molecules adsorbed at any two of the same three sites, which gives rise to the three orientations of the curved feature; and (iii) the oval feature to a single dissociated water molecule. This is summarized in Table 1. Also consistent with the experiments are the relative orientations of the curved features and the bright triangles with respect to the orientation of the characteristic dark triangles of the water-free surface. Furthermore, the corrugation profiles in Figure 6 indicate a much higher apparent height for the triangles than for the curved features, as observed in the experiment as well. Finally,

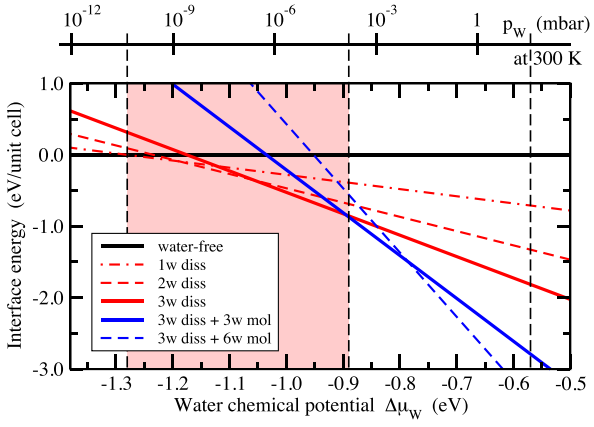

Figure 7. Surface phase diagram of the $In_2O_3(111)$ surface as a function of the water chemical potential. In the top *x*-axis, the chemical potential has been converted to a water partial pressure scale for the temperature of 300 K. The red-shaded area shows the stability range of hydroxylated surfaces structures by water dissociation. The vertical dashed black line at −0.57 eV indicates the chemical potential of liquid water at RT.[35]

Table 1. Features Observed in STM Images upon Water Adsorption on $In_2O_3(111)$

oval	single dissociated water molecule, *i.e.*, OH^- and H^+ sitting in close vicinity forming O_WH and O_SH
curved feature	two dissociated water molecules, *i.e.*, two ovals enclosing 120°
curved feature with dot	two dissociated water molecules + single O_WH (the H of an O_SH is removed by the tip)
bright triangle	three dissociated water molecules

DOI: 10.1021/acsnano.7b06387
ACS Nano 2017, 11, 11531−11541

full dissociation (*i.e.*, no molecular adsorption) and a saturation coverage of three water molecules per surface unit cell (6 OH groups) are both in full agreement with the XPS measurements.

Additional DFT calculations were performed to understand the results of the tip-induced manipulations of the saturated water layer (see Figure 5). In the STM images, the saturated water layer is formed by bright triangles, consisting of six OH groups (three O_SH and three O_WH) from three dissociated water molecules. Upon stripping off species with the STM tip, the bright triangle converts into the curved species with a dot next to it. The curved features have already been identified to consist of two dissociated water molecules. Thus, the obvious explanation of the STM images is that one OH group or its hydrogen atom has been removed by the tip-induced manipulations and the remaining other OH group from the third dissociated water molecule is now visible as a dot next to the curved feature. However, the question remains as to which OH group has been removed or altered and which OH group (O_SH or O_WH) remains on the surface after the tip-induced manipulations. From the STM images, the adsorption site of the dot is positioned in the In(5c) region, suggesting that the proton from the O_SH is missing.

To address this question thoroughly, DFT calculations were started from the structure with three dissociated water molecules, which is initially imaged as a bright triangle (compare Figures 5a, 6c, and 8a). From this structure, either

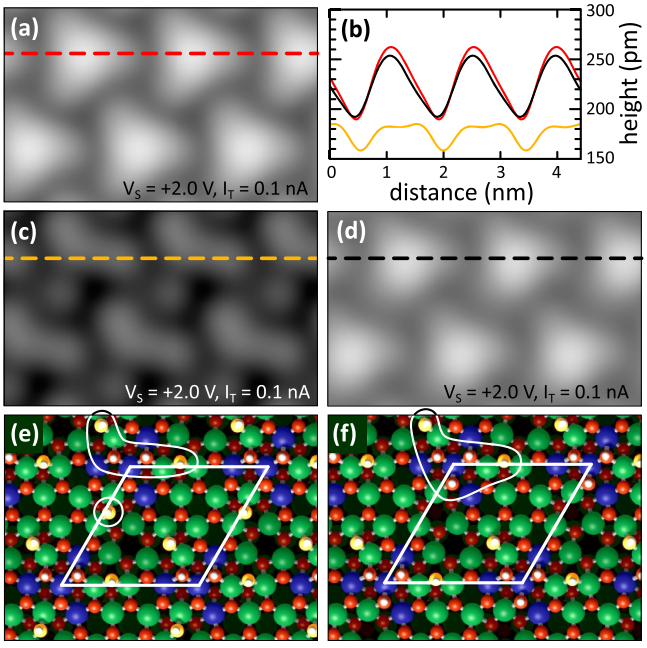

Figure 8. DFT calculations of vacancies in the hydroxyl layer. (a) Undisturbed surface with three dissociated water molecules per unit cell. (b) Height profiles taken from (a–d). (c,d) STM contrasts of the structures in (e,f), calculated using the Bardeen approach. (e,f) Atomic models, after the removal of (e) one H from an O_SH group and (f) one O_WH group per unit cell, respectively.

the terminal O_WH unit or the proton from the O_SH group was removed, see Figure 8e,f. The corresponding STM images for the relaxed structures are shown in Figure 8c,d together with representative line scans in panel (b). From these images and the line scans, we can directly conclude that the proton of one of the three O_SH groups has been removed in the STM experiments. Only in this case (Figure 8c,e), the remaining OH group (O_WH) appears as a distinct dot next to the curved feature in the STM image. Furthermore, the apparent height of the whole structure is significantly reduced as observed in the experiment. The reason is that removing a neutral H atom also removes an electron from the surface and thus creates a hole in the valence band. This corresponds to a p-type defect (acceptor) with a locally reduced electron density. The removal of a H atom is actually equivalent to the addition of a neutral OH to the surface, which accepts an electron from the surface to become a negatively charged OH^-. Such p-type defects in semiconductors are commonly imaged as depressions in empty states.[36] In contrast, removing a terminal O_WH group leaves the STM image and the associated corrugation profile almost unchanged (see Figure 8b,d). The remaining O_SH group is too close to the other four OH groups of the curved feature so that it cannot be resolved as a separate dot in the STM image. Furthermore, by removing a neutral O_WH group, an n-type defect is formed that locally increases the electron density due to the donation of an electron. Similar as before, the removal of the O_WH leaves a neutral H atom from the dissociated water molecule behind, which acts as an electron donor. The increase in the electron density compensates the loss in geometrical height, so that the apparent height remains almost unchanged, which would contradict the experimental observation.

DISCUSSION

In this combined STM/XPS and DFT study, we demonstrate that single water molecules adsorb dissociatively on the In_2O_3(111) surface, forming two types of OH groups, O_WH and O_SH. The energetically most favored adsorption site for the H^+ is one of the O(3c) bridging to two In(6c) atoms and one In(5c) (see Figure 6). The OH^- adsorbs directly next to the proton, bridging two In(5c) atoms; one of these In(5c) is shared with the O(3c) where the proton adsorbs. The adsorption of the O_WH also leads to a local distortion (*i.e.*, lifting of the relaxation) of the surface by pulling these two (former) In(5c) closer together, resulting in a decrease of 0.48 Å from their relaxed distance of 4.08 Å. The symmetry of the surface offers three equivalent adsorption sites per unit cell that are occupied with decreasing adsorption energies per water molecule due to a substrate-mediated effective repulsion as discussed earlier. The surface gets saturated once these sites are occupied, leading to bright triangular features in the STM images. Additional water molecules cannot adsorb on the surface at RT in UHV, as observed experimentally, which is also reflected in the DFT adsorption energies of additional water molecules.

Moreover, this demonstrates that the unit cell of the In_2O_3(111) surface is heterogeneous in terms of reactivity, and the dissociation takes place on lattice sites of the intact surface, without any preference for step edges or defective regions on the surface. In_2O_3 is a complex oxide with a large bulk unit cell due to ordered anion vacancies in the fluorite lattice (bixbyite structure). The unit cell of the (111) surface features four inequivalent types of 3-fold coordinated surface oxygen atoms, O(3c), each represented by three atoms—but only one type is involved in the proton adsorption. The reactivity of these O(3c) atoms is determined by the coordination of their neighboring In atoms, and those sharing bonds with two In(6c) and one In(5c) are the most reactive, while the remaining three different types of O(3c) surrounded mostly by In(5c) do not contribute to this reaction. The four In(6c) atoms are not evenly distributed within the surface unit

DOI: 10.1021/acsnano.7b06387
ACS Nano 2017, 11, 11531–11541

cell (which contains 16 In atoms in total); instead they are clustered, resulting in the heterogeneous reactivity.

The surface is saturated after the adsorption of three molecules per unit cell, which results in a rather low coverage/density of OH groups considering the size of the unit cell and the number of surface oxygen atoms; it corresponds to 1.7×10^{14} cm^{-2} dissociated water molecules or 3.4×10^{14} cm^{-2} OH groups (counting both O_WH and O_SH). At RT, even a very small amount of water in the pristine UHV environment at base pressures $<2 \times 10^{-10}$ mbar is sufficient to saturate the surface completely within a few hours.

While water dissociation on an oxide at RT is not entirely surprising, the observation of water molecules not dissociated at defects but at regular lattice sites at temperatures as low as 100 K is unusual, and the formation of a well-ordered and almost defect-free hydroxyl layer is intriguing. Defects always found in the hydroxyl layer are partial vacancies where one water molecule ($O_WH^- + H^+$) or a H atom is missing. This can be explained either by a slightly elevated sample temperature during the water exposure due to the previous sample heating, or a defect in the $In_2O_3(111)$ lattice [*e.g.*, a missing O(3c) and thus less In(6c)]. The hydroxylation on $In_2O_3(111)$ is self-limited, as the OH groups block the reactive sites. Apart from some relaxations of the substrate, the OH groups do not change their adsorption sites or structure depending on the water coverage. According to the phase diagram in Figure 7, molecular water is expected to form ordered structures on top of the hydroxyl layer, although only at temperatures below RT or high partial pressures. This is also reflected in the binding energy of the molecular species discussed earlier, and the XPS data obtained at 100 K. Similar temperature dependencies for molecular adsorption of single water molecules are found on other oxides, although dissociation may still occur at defect sites such as O vacancies,[37] due to water−water interaction or "unsuitable" atomic distances for molecular adsorption on the surface.[11] Dense structures formed at low temperatures have been found to be either purely molecular or of a mixed nature. A peculiar example is $ZnO(10\bar{1}0)$, where a purely molecular phase coexists with a mixed phase that is formed by water molecules which are constantly dissociating and recombining.[9]

The predominant investigation technique used in this work is low-temperature STM, in particular, taking advantage of local manipulations of the surface with the STM tip. The quantitative simulations in Figures 6 and 8 provide a clear interpretation of the resulting structures. Water-related species are desorbed by single voltage pulses (the proton from the O_SH) with the STM tip as well as by scanning larger areas at a high bias voltage (the proton from the O_SH of the saturated surface and both the O_WH and the proton from low coverages; see Supporting Information). We have strong indications that the desorption of the proton can be realized purely by the electric field, as we get the same results by applying the voltage pulse using a conducting STM or a noncontact AFM tip with an insulating particle at the tip apex. During the past decade, such controlled manipulations have been developed as a valuable tool to identify and differentiate adsorbed surface entities with atomic-scale precision, for example, by their charge state,[38] as well as subsurface species, such as oxygen vacancies in anatase TiO_2.[39] Furthermore, such manipulations allow us to study the tip−adsorbate and adsorbate−surface interactions and to trigger single chemical reactions.[40] Classified by the mechanism, STM manipulations operate *via* forces (pushing, pulling, sliding),[41] electric field (field evaporation and diffusion),[40] or electric current (inelastic tunneling, vibrational and electronic excitations).[38,42] The manipulation of weakly interacting species, such as water molecules on metals and oxide surfaces, usually succeeds by tuning the electric field between the tip and surface, *via* inelastic tunneling, or a combination of both.[43] It has been demonstrated that such manipulations allow controlled studies of water diffusion,[7,44] clustering,[44,45] dissociation,[7,46,47] and desorption.[47]

The selective desorption of one H per unit cell from the saturated surface was vital for unraveling the configuration of the water-related features and, together with DFT calculations, provides detailed information on the adsorption sites and geometry of the dissociated water overlayer. The desorption of one proton from one of the three O_SH could be confirmed by DFT calculations by reproducing the "fingerprint" of the manipulated area, that is, the observed features combined with the change in contrast due to local band bending at the p-type defect. The different features seen at low water coverage in the STM images as well as after the described manipulation are summarized in Table 1. They correspond to 1, 2, 2.5 (manipulated), and 3 split water molecules adsorbed at the same dark triangle [same In(6c)/O(3c) region of the unit cell].

CONCLUSIONS

In this work, we present the hydroxylation of $In_2O_3(111)$ *via* water exposure at room temperature as investigated with STM, XPS, and DFT methods. Indium oxide is a material that has been commonly used in devices for more than three decades, and it is surprising that its reactivity toward water has not previously been thoroughly studied. Even more surprisingly, the $In_2O_3(111)$ surface (despite its complex crystal structure and unit cell) behaves like a "textbook example" when exposed to water: A well-ordered hydroxyl layer with (1×1) symmetry is formed, where both the OH^- and H^+ remain at the surface as O_WH and O_SH groups, respectively. The saturation coverage corresponds to three dissociated water molecules per unit cell, the dissociation takes place at lattice sites, and all of the O_WH and O_SH occupy equivalent sites. This demonstrates that only 1/4 of the surface oxygen atoms O(3c) are involved in the water dissociation and proton adsorption, with their reactivity being determined by the coordination of the neighboring In atoms. The reactive sites are not evenly distributed within the unit cell but located close to each other, making the unit cell heterogeneous in terms of reactivity. Moreover, the OH groups do not diffuse or rearrange but block the reactive dissociation sites, thereby limiting the maximum degree of surface hydroxylation. The result is a well-defined and stable hydroxyl layer covering the entire surface with a surprisingly low saturation coverage.

METHODS

The STM measurements were performed using two different UHV systems: one equipped with a low-temperature STM (Omicron LT-STM) operating at 79 and 5 K and the other one with a room temperature STM (Omicron STM-1). The LT-STM system consists of an analysis chamber (base pressure 5×10^{-12} mbar) and an adjacent preparation chamber (base pressure 7×10^{-11} mbar). The STM-1 is housed in a smaller one-chamber system with a base pressure of 2×10^{-10} mbar. Electrochemically etched W tips were cleaned by sputtering, and the metallic behavior of the tip was frequently restored *in situ* on auxiliary Au(110) and Cu(100) single crystals. XPS measurements in grazing emission (60°/65° off the surface normal) were conducted using both a conventional X-ray source in the LT-

DOI: 10.1021/acsnano.7b06387
ACS Nano 2017, 11, 11531−11541

STM chamber (Mg Kα radiation, 1253.6 eV) and synchrotron radiation at the beamline I311 of the Maxlab II facility in Lund, Sweden.

A glass tube with a few drops of distilled water (Milli-Q) was attached to the UHV systems *via* a high-precision leak valve. The tube was also connected *via* a separate pumping line to a turbo-molecular pump. Prior to the experiments, the water was cleaned by several freeze−pump−thaw cycles and finally checked with a mass spectrometer for cleanliness. In the LT-STM chamber, the crystal was held at 100 K while exposed to water vapor in the preparation chamber (*i.e., in situ* dosing during the XPS measurements); in the RT-STM, water was dosed while scanning. During water exposure, the pressure was kept below 5×10^{-9} mbar. Included in the quoted values is inadvertent dosing from the residual vacuum after closing the leak valve.

The In_2O_3 single crystals were grown at the Oak Ridge National Laboratory using the flux method. The cubic (001)-oriented crystals have a size of 1−3 mm.[48] They were oriented and cut-polished by the company SurfaceNet. The $In_2O_3(111)$ surface was cleaned by several cycles of sputtering with Ar^+ ions (1 keV) followed by annealing at 450−500 °C either in UHV or O_2. The last annealing step was always carried out in O_2 including a cool down to 150 °C that leads to atomically flat surfaces with a relaxed bulk-truncated and stoichiometric surface structure. As described in ref 29, a more reducing treatment in UHV results in excess In adatoms on the surface. The O_2 pressure (backfill) necessary to suppress adatom formation varies between $(1-6) \times 10^{-7}$ mbar, depending on the UHV chamber setup. The appearance of the clean $In_2O_3(111)$ surface in the STM is described in the same ref 29. The STM images presented in this work were measured on several crystals, at RT, 79 K, and 5 K, all showing the same features upon water adsorption and manipulation.

DFT calculations were carried out with the periodic plane-wave code PWscf of the Quantum Espresso software package,[49] using the Perdew−Burke−Ernzerhof exchange-correlation functional,[50] Vanderbilt ultrasoft pseudopotentials,[51] and a plane-wave kinetic energy cutoff of 30 Ry. The surface structures were represented by periodically repeated slabs with a thickness of four $O_{12}-In_{16}-O_{12}$ triple layers and a primitive (1×1) surface unit cell. The supercell for the stoichiometric water-free surface thus contained 160 atoms. The atoms in the bottom half of the slab were kept fixed at their bulk positions, whereas the atoms in the top half and the adsorbed water molecules were relaxed until a force convergence threshold of 5 meV/Å for the largest residual force component was reached. A $(2 \times 2 \times 1)$ Monkhorst−Pack *k*-point mesh for Brillouin zone integrations was sufficient for obtaining well-converged energies and geometries. For more details on the computational setup, see refs 29 and 30.

The STM images and STM line profiles were determined by evaluating Bardeen's tunneling formula using our own implementation.[52] The advantage of this approach is that the STM tunneling current for a given position of the tip above the substrate is calculated fully *ab initio*, without any adjustable parameter, from the tip and the substrate wave functions. This allows a direct, quantitative comparison to be made between the calculated and measured STM height profiles. The STM tip was modeled by a small pyramid of five tungsten atoms supported on a (100)-oriented tungsten slab. All images represent constant-current conditions, that is, the brightness reflects the height of the STM tip above the surface for a given current.

ASSOCIATED CONTENT

Supporting Information

The Supporting Information is available free of charge on the ACS Publications website at DOI: 10.1021/acsnano.7b06387.

Additional experimental data: O1s XPS, STM of the water multilayer, and STM with high bias voltage; additional DFT calculations: atomic and electronic structure of the adsorbate-free surface, and alternative configurations for one, two, and three adsorbed water molecules (PDF)

AUTHOR INFORMATION

Corresponding Author

*E-mail: wagner@iap.tuwien.ac.at.

ORCID

Margareta Wagner: 0000-0001-9414-1696
Zhiming Wang: 0000-0002-4854-2170
Bernd Meyer: 0000-0002-3481-8009
Ulrike Diebold: 0000-0003-0319-5256

Notes

The authors declare no competing financial interest.

ACKNOWLEDGMENTS

M.W. gratefully acknowledges the FWF project T759-N27. S.S. thanks the Fonds der Chemischen Industrie (FCI) for a Chemiefonds Fellowship. P.L. and M.S. acknowledge support from FWF project F4505, and R.B. acknowledges support from the FWF doctoral college "Solids4fun (W1243)". Research at the Oak Ridge National Laboratory for L.B. was sponsored by the U.S. Department of Energy, Basic Energy Sciences, Materials Sciences and Engineering Division (DE-AC05-00OR22725). U.D. acknowledges supported by the European Research Council (Advanced Grant "OxideSurfaces" ERC-2011-ADG_20110209).

REFERENCES

(1) Dohnálek, Z.; Lyubinetsky, I.; Rousseau, R. Thermally-Driven Processes on Rutile $TiO_2(110)$-(1×1): A Direct View at the Atomic Scale. *Prog. Surf. Sci.* **2010**, *85*, 161−205.

(2) Lee, J.; Sorescu, D. C.; Deng, X.; Jordan, K. D. Water Chain Formation on $TiO_2(110)$. *J. Phys. Chem. Lett.* **2013**, *4*, 53−57.

(3) Herman, G. S.; Dohnálek, Z.; Ruzycki, N.; Diebold, U. Experimental Investigation of the Interaction of Water and Methanol with Anatase-$TiO_2(101)$. *J. Phys. Chem. B* **2003**, *107*, 2788−2795.

(4) Setvin, M.; Daniel, B.; Aschauer, U.; Hou, W.; Li, Y.-F.; Schmid, M.; Selloni, A.; Diebold, U. Identification of Adsorbed Molecules *via* STM Tip Manipulation: CO, H_2O, and O_2 on TiO_2 Anatase (101). *Phys. Chem. Chem. Phys.* **2014**, *16*, 21524−21530.

(5) Torbrügge, S.; Custance, O.; Morita, S.; Reichling, M. Manipulation of Individual Water Molecules on $CeO_2(111)$. *J. Phys.: Condens. Matter* **2012**, *24*, 084010.

(6) Fester, J.; García-Melchor, M.; Walton, A. S.; Bajdich, M.; Li, Z.; Lammich, L.; Vojvodic, A.; Lauritsen, J. V. Edge Reactivity and Water-Assisted Dissociation on Cobalt Oxide Nanoislands. *Nat. Commun.* **2017**, *8*, 14169.

(7) Shin, H.-J.; Jung, J.; Motobayashi, K.; Yanagisawa, S.; Morikawa, Y.; Kim, Y.; Kawai, M. State-Selective Dissociation of a Single Water Molecule on an Ultrathin MgO Film. *Nat. Mater.* **2010**, *9*, 442−447.

(8) Meyer, B.; Marx, D.; Dulub, O.; Diebold, U.; Kunat, M.; Langenberg, D.; Wöll, C. Partial Dissociation of Water Leads to Stable Superstructures on the Surface of Zinc Oxide. *Angew. Chem., Int. Ed.* **2004**, *43*, 6641−6645.

(9) Dulub, O.; Meyer, B.; Diebold, U. Observation of the Dynamical Change in a Water Monolayer Adsorbed on a ZnO Surface. *Phys. Rev. Lett.* **2005**, *95*, 136101.

(10) Halwidl, D.; Stöger, B.; Mayr-Schmölzer, W.; Pavelec, J.; Fobes, D.; Peng, J.; Mao, Z.; Parkinson, G. S.; Schmid, M.; Mittendorfer, F.; Redinger, J.; Diebold, U. Adsorption of Water at the SrO Surface of Ruthenates. *Nat. Mater.* **2015**, *15*, 450−455.

(11) Mu, R.; Zhao, Z.-J.; Dohnálek, Z.; Gong, J. Structural Motifs of Water on Metal Oxide Surfaces. *Chem. Soc. Rev.* **2017**, *46*, 1785−1806.

(12) King, P. D. C.; Veal, T. D.; Fuchs, F.; Wang, C. Y.; Payne, D. J.; Bourlange, A.; Zhang, H.; Bell, G. R.; Cimalla, V.; Ambacher, O.; Egdell, R. G.; Bechstedt, F.; McConville, C. F. Band Gap, Electronic Structure, and Surface Electron Accumulation of Cubic and

DOI: 10.1021/acsnano.7b06387
ACS Nano 2017, 11, 11531−11541

Rhombohedral In_2O_3. *Phys. Rev. B: Condens. Matter Mater. Phys.* **2009**, *79*, 205211.
(13) King, P. D. C.; Veal, T. D.; Payne, D. J.; Bourlange, A.; Egdell, R. G.; McConville, C. F. Surface Electron Accumulation and the Charge Neutrality Level in In_2O_3. *Phys. Rev. Lett.* **2008**, *101*, 116808.
(14) Phipps, G.; Mikolajczak, C.; Guckes, T. Indium and Gallium: Long-Term Supply. *Renew. Energy Focus* **2008**, *9*, 56.
(15) Egdell, R. G. Dopant and Defect Induced Electronic States at In_2O_3 Surfaces. In *Defects at Oxide Surfaces 58*; Jupille, J., Thornton, G., Eds.; Springer International: New York, 2015; p 351.
(16) Klein, A.; Körber, C.; Wachau, A.; Säuberlich, F.; Gassenbauer, Y.; Harvey, S. P.; Proffit, D. E.; Mason, T. O. Transparent Conducting Oxides for Photovoltaics: Manipulation of Fermi Level, Work Function and Energy Band Alignment. *Materials* **2010**, *3*, 4892−4914.
(17) Martin, O.; Martín, A. J.; Mondelli, C.; Mitchell, S.; Segawa, T. F.; Hauert, R.; Drouilly, C.; Curulla-Ferré, D.; Pérez-Ramírez, J. Indium Oxide as a Superior Catalyst for Methanol Synthesis by CO_2 Hydrogenation. *Angew. Chem.* **2016**, *128*, 6369−6373.
(18) Liu, Y.; Mustain, W. E. High Stability, High Activity Pt/ITO Oxygen Reduction Electrocatalysts. *J. Am. Chem. Soc.* **2013**, *135*, 530−533.
(19) Fan, J. C. C.; Goodenough, J. B. X-Ray Photoemission Spectroscopy Studies of Sn-doped Indium-Oxide Films. *J. Appl. Phys.* **1977**, *48*, 3524.
(20) Donley, C.; Dunphy, D.; Paine, D.; Carter, C.; Nebesny, K.; Lee, P.; Alloway, D.; Armstrong, N. R. Characterization of Indium-Tin Oxide Interfaces Using X-ray Photoelectron Spectroscopy and Redox Processes of a Chemisorbed Probe Molecule: Effect of Surface Pretreatment Conditions. *Langmuir* **2002**, *18*, 450−457.
(21) Janowitz, C.; Scherer, V.; Mohamed, M.; Krapf, A.; Dwelk, H.; Manzke, R.; Galazka, Z.; Uecker, R.; Irmscher, K.; Fornari, R.; Michling, M.; Schmeißer, D.; Weber, J. R.; Varley, J. B.; Van de Walle, C. G. Experimental Electronic Structure of In_2O_3 and Ga_2O_3. *New J. Phys.* **2011**, *13*, 085014.
(22) Kim, J. S.; Ho, P. K. H.; Thomas, D. S.; Friend, R. H.; Cacialli, F.; Bao, G.-W.; Li, S. F. Y. X-ray Photoelectron Spectroscopy of Surface-Treated Indium-Tin Oxide Thin Films. *Chem. Phys. Lett.* **1999**, *315*, 307−312.
(23) Brinzari, V.; Korotcenkov, G.; Ivanov, M.; Nehasil, V.; Matolin, V.; Mašek, K.; Kamei, M. Valence Band and Band Gap Photoemission Study of (111) In_2O_3 Epitaxial Films Under Interactions with Oxygen, Water and Carbon Monoxide. *Surf. Sci.* **2007**, *601*, 5585−5594.
(24) Atashbar, M. Z.; Gong, B.; Sun, H. T.; Wlodarski, W.; Lamb, R. Investigation on Ozone-Sensitive In_2O_3 Thin Films. *Thin Solid Films* **1999**, *354*, 222−226.
(25) Kościelniak, P.; Grzeszczak, A.; Szuber, J. XPS and AFM Studies of Surface Chemistry and Morphology of In_2O_3 Ultrathin Films Deposited by Rheotaxial Growth and Vacuum Oxidation After Air Exposure. *Cryst. Res. Technol.* **2015**, *50*, 884−890.
(26) Himmerlich, M.; Eisenhardt, A.; Berthold, T.; Wang, C. Y.; Cimalla, V.; Ambacher, O.; Krischok, S. Interaction of Indium Oxide Nanoparticle Film Surfaces with Ozone, Oxygen and Water. *Phys. Status Solidi A* **2016**, *213*, 831−838.
(27) Detweiler, Z. M.; Wulfsberg, S. M.; Frith, M. G.; Bocarsly, A. B.; Bernasek, S. L. The Oxidation and Surface Speciation of Indium and Indium Oxides Exposed to Atmospheric Oxidants. *Surf. Sci.* **2016**, *648*, 188−195.
(28) Agoston, P.; Albe, K. Thermodynamic Stability, Stoichiometry, and Electronic Structure of bcc-In_2O_3 Surfaces. *Phys. Rev. B: Condens. Matter Mater. Phys.* **2011**, *84*, 045311.
(29) Wagner, M.; Seiler, S.; Meyer, B.; Boatner, L. A.; Schmid, M.; Diebold, U. Reducing the $In_2O_3(111)$ Surface Results in Ordered Indium Adatoms. *Adv. Mater. Interfaces* **2014**, *1*, 1400289.
(30) Wagner, M.; Lackner, P.; Seiler, S.; Gerhold, S.; Osiecki, J.; Schulte, K.; Boatner, L. A.; Schmid, M.; Meyer, B.; Diebold, U. Well-Ordered In Adatoms at the $In_2O_3(111)$ Surface Created by Fe Deposition. *Phys. Rev. Lett.* **2016**, *117*, 206101.
(31) Morales, E. H.; He, Y.; Vinnichenko, M.; Delley, B.; Diebold, U. Surface Structure of Sn-Doped In_2O_3 (111) Thin Films by STM. *New J. Phys.* **2008**, *10*, 125030.
(32) Thiel, P. A.; Madey, T. E. The Interaction of Water with Solid Surfaces: Fundamental Aspects. *Surf. Sci. Rep.* **1987**, *7*, 211−385.
(33) Silber, D.; Kowalski, P. M.; Traeger, F.; Buchholz, M.; Bebensee, F.; Meyer, B.; Wöll, C. Adsorbate-Induced Lifting of Substrate Relaxation is a General Mechanism Governing Titania Surface Chemistry. *Nat. Commun.* **2016**, *7*, 12888.
(34) Meyer, B.; Rabaa, H.; Marx, D. Water Adsorption on ZnO($10\bar{1}0$) from Single Molecules to Partially Dissociated Monolayers. *Phys. Chem. Chem. Phys.* **2006**, *8*, 1513.
(35) Bauer, T.; Schmaltz, T.; Lenz, T.; Halik, M.; Meyer, B.; Clark, T. Phosphonate- and Carboxylate-Based Self-Assembled Monolayers for Organic Devices: A Theoretical Study of Surface Binding on Aluminum Oxide with Experimental Support. *ACS Appl. Mater. Interfaces* **2013**, *5*, 6073−6080.
(36) Domke, C.; Ebert, P.; Heinrich, M.; Urban, K. Microscopic Identification of the Compensation Mechanisms in Si-Doped GaAs. *Phys. Rev. B: Condens. Matter Mater. Phys.* **1996**, *54*, 10288.
(37) Salmeron, M.; Bluhm, H.; Tatarkhanov, M.; Ketteler, G.; Shimizu, T. K.; Mugarza, A.; Deng, X.; Herranz, T.; Yamamoto, S.; Nilsson, A. Water Growth on Metals and Oxides: Binding, Dissociation and Role of Hydroxyl Groups. *Faraday Discuss.* **2009**, *141*, 221−229.
(38) Repp, J.; Meyer, G.; Olsson, F. E.; Persson, M. Controlling the Charge State of Individual Gold Adatoms. *Science* **2004**, *305*, 493.
(39) Setvín, M.; Schmid, M.; Diebold, U. Aggregation and Electronically Induced Migration of Oxygen Vacancies in TiO_2 Anatase. *Phys. Rev. B: Condens. Matter Mater. Phys.* **2015**, *91*, 195403.
(40) Setvín, M.; Aschauer, U.; Hulva, J.; Simschitz, T.; Daniel, B.; Schmid, M.; Selloni, A.; Diebold, U. Following the Reduction of Oxygen on TiO_2 Anatase (101) Step by Step. *J. Am. Chem. Soc.* **2016**, *138*, 9565−9571.
(41) Bartels, L.; Meyer, G.; Rieder, K.-H. Basic Steps of Lateral Manipulation of Single Atoms and Diatomic Clusters with a Scanning Tunneling Microscope Tip. *Phys. Rev. Lett.* **1997**, *79*, 697.
(42) Kim, Y.; Motobayashi, K.; Frederiksen, T.; Ueba, H.; Kawai, M. Action Spectroscopy for Single-Molecule Reactions − Experiments and Theory. *Prog. Surf. Sci.* **2015**, *90*, 85−143.
(43) Guo, J.; Bian, K.; Lin, Z.; Jiang, Y. Perspective: Structure and Dynamics of Water at Surfaces Probed by Scanning Tunneling Microscopy and Spectroscopy. *J. Chem. Phys.* **2016**, *145*, 160901.
(44) Mitsui, T.; Rose, M. K.; Fomin, E.; Ogletree, D. F.; Salmeron, M. Water Diffusion and Clustering on Pd(111). *Science* **2002**, *297*, 1850.
(45) Morgenstern, K.; Rieder, K.-H. Formation of the Cyclic Ice Hexamer *via* Excitation of Vibrational Molecular Modes by the Scanning Tunneling Microscope. *J. Chem. Phys.* **2002**, *116*, 5746.
(46) Kumagai, T.; Kaizu, M.; Okuyama, H.; Hatta, S.; Aruga, T.; Hamada, I.; Morikawa, Y. Tunneling Dynamics of a Hydroxyl Group Adsorbed on Cu(110). *Phys. Rev. B: Condens. Matter Mater. Phys.* **2009**, *79*, 035423.
(47) Mugarza, A.; Shimizu, T. K.; Ogletree, D. F.; Salmeron, M. Chemical Reactions of Water Molecules on Ru(0001) Induced by Selective Excitation of Vibrational Modes. *Surf. Sci.* **2009**, *603*, 2030−2036.
(48) Hagleitner, D. R.; Menhart, M.; Jacobson, P.; Blomberg, S.; Schulte, K.; Lundgren, E.; Kubicek, M.; Fleig, J.; Kubel, F.; Puls, C.; Limbeck, A.; Hutter, H.; Boatner, L. A.; Schmid, M.; Diebold, U. Bulk and Surface Characterization of In_2O_3(001) Single Crystals. *Phys. Rev. B: Condens. Matter Mater. Phys.* **2012**, *85*, 115441.
(49) Giannozzi, P.; Baroni, S.; Bonini, N.; Calandra, M.; Car, R.; Cavazzoni, C.; Ceresoli, D.; Chiarotti, G. L.; Cococcioni, M.; Dabo, I.; Dal Corso, A.; de Gironcoli, S.; Fabris, S.; Fratesi, G.; Gebauer, R.; Gerstmann, U.; Gougoussis, C.; Kokalj, A.; Lazzeri, M.; Martin-Samos, L.; et al. QUANTUM ESPRESSO: A Modular and Open-Source Software Project for Quantum Simulations of Materials. *J. Phys.: Condens. Matter* **2009**, *21*, 395502.

DOI: 10.1021/acsnano.7b06387
ACS Nano 2017, 11, 11531−11541

(50) Perdew, J. P.; Burke, K.; Ernzerhof, M. Generalized Gradient Approximation Made Simple. *Phys. Rev. Lett.* **1996**, *77*, 3865−3868; Erratum: *Phys. Rev. Lett.* **1997**, *78*, 1396.
(51) Vanderbilt, D. Soft Self−Consistent Pseudopotentials in a Generalized Eigenvalue Formalism. *Phys. Rev. B: Condens. Matter Mater. Phys.* **1990**, *41*, 7892−7895.
(52) Kovacik, R.; Meyer, B.; Marx, D. F−Centers *versus* Dimer Vacancies on ZnO Surfaces: Characterization by STM and STS Calculations. *Angew. Chem., Int. Ed.* **2007**, *46*, 4894−4897.

DOI: 10.1021/acsnano.7b06387
ACS Nano 2017, 11, 11531−11541